Article:

Liu, Q. and Ball, E.A. (2021) The meta distribution of the SIR for LoRaWANs with power control. IEEE Transactions on Industrial Informatics, 17 (4). pp. 2579-2586. ISSN 1551-3203

https://doi.org/10.1109/tii.2020.3003474

The meta distribution of the SIR for LoRaWANs with power control

***Abstract*—To reduce energy consumption, a device in a LoRa (Long Range) wide area network (LoRaWAN) needs to adjust its transmit power according to the distance from its tagged Gateway (GW). It is important to measure the performance of the LoRaWANs uplink with power control. In this paper, we focus on the analysis of the coverage probability and the meta distribution of the signal-to-interference ratio (SIR) for a LoRaWAN uplink with fractional power control (FPC). The LoRaWAN uplink is analysed based on the Poisson point process (PPP). We present the possible reductions in transmit power of devices whilst ensuring that the received signal power is greater than the receiver sensitivity. We derive the coverage probability of a LoRaWAN uplink, and show how power control influences it. Finally, utilizing the meta distribution of SIR, the fine-grained information of the LoRaWAN is revealed. The results show that the power control greatly increases the successful probability of edge-devices with little effect on the probability of inner-devices if an appropriate FPC coefficient is chosen. This is because the LoRa signal can be demodulated at a very low required SIR threshold.**

***Index Terms*—LoRaWAN, Poisson point process, Power control, Uplink, Meta distribution**

I. Introduction

A. Motivation

More and more devices used across various fields are connected to the Internet. Many reports forecast that the Internet of Things (IoT) smart objects are expected to reach 212 billion entities deployed globally by the end of 2020. By 2022, machine-to-machine (M2M) traffic flows are expected to constitute up to 45% of the whole Internet traffic. The whole annual economic impact caused by the IoT is estimated to be in the range of 2.7 trillion to 6.2 trillion by 2025 [1]–[4].

An important branch of IoT networks is low-power wide area network (LPWAN) [5], which is designed for massive numbers of devices connecting from long distance with low traffic. There are three typical LPWAN technologies: narrow-band Internet of Things (NB-IoT), long range wide area network (LoRaWAN), and SigFox. As a part of the 3rd Generation Partnership Project (3GPP) $Release13$, NB-IoT is designed to be compatible with Long Term Evolution (LTE) but kept as simple as possible in order to reduce hardware costs and minimize battery consumption [6]. NB-IoT devices directly communicate with base stations (BSs), i.e. eNBs, thus most of the research results on cellular networks can be directly used for NB-IoT networks. Both LoRaWAN devices and Sigfox devices can be organized by Gateways (GWs) which are deployed by users. These devices access to the networks independently at a randomly chosen sub-channel based on pure Aloha protocol in uplink. Comparing to NB-IoT, LoRaWAN and Sigfox can be deployed quickly with less cost for some use-case applications, especially where devices do not move after deployment.

NB-IoT is compatible with cellular networks and Sigfox is more simple than LoRaWANs, we only consider LoRaWANs in this paper. With the rapid growth of IoT market, LoRaWAN as one of LPWAN technologies has been becoming more and more popular due to the following factors: massive device connectivity, the lower required signal-to-noise ratio (SNR) for demodulation, simple network protocol, and usage of the industrial scientific medical (ISM) band. But there has been less research on LoRaWAN networks performance metrics. Furthermore, in many applications it is desirable for the devices to work for 10 years, supplied by a primary battery. To guide the deployment of rapidly developing LoRaWANs and save energy, it is now necessary to adopt a good mathematical model to analyse the LoRaWANs and also consider power control.

B. Related work

In recent years, stochastic geometry has been widely accepted to model and analyse wireless networks with randomly placed nodes. Notably, the Poisson point process (PPP) is the most tractable model for analysis of cellular networks due to the simple form of its probability generating functional (PGFL) [7, Theorem 4.9]. Most of the prior works focus on the standard success (coverage) probability as the performance metric [8]–[15]. The coverage probability is the spatial averaging over the channel fading and the point process, and gives some basic information on the signal-to-interference ratio (SIR) performance. To obtain more fine-grained information on an individual link such as the proportion of users in a Poisson network archiving a desired link reliability with a given SIR threshold, or the differences of two networks with the same coverage probability, the meta distribution of the SIR was proposed as a general concept and analysed for Poisson bipolar and cellular networks in [16].

The results of PPP uplink cellular networks can be directly used for NB-IoT networks because of their compatibility with cellular networks, but are not suitable for LoRaWAN. In uplink cellular networks, there is at most one user equipment in each cell accessing the network in a particular time-frequency resource block (RB). In LoRaWANs, each active device independently sends messages to its tagged GW at a randomly chosen sub-channel. To analyse LPWANs based on PPP, in [17], a “card tossing” model was proposed to analyse the interference of 2-dimensional (time-frequency) plane in LPWANs. A special Aloha network, the bipolar model, was studied in [18]. The authors derived the density of successful transmissions and the density of throughput exploiting a PPP model. The results of Aloha bipolar networks can not be directly used in LoRaWANs because all pairs of devices and GWs have the same distance in bipolar Aloha network.

Moreover, in IoT networks, the devices may transmit data with power control for power saving and mitigating the interference. Many existing works about power control focus on cellular uplink networks. An inter-cell interference coordination method using coordinated inter-cell interference power control in uplink cellular networks was proposed in [19]. A truncated channel inversion power control model was proposed based on stochastic geometry for cellular uplink transmission in [20]. The authors analysed the outage probability and spectral efficiency in both single and multi-tier cellular wireless networks exploiting the PPP model. In [21], the authors modelled and analysed the meta distribution of the SIR for cellular networks with power control based on non-homogeneous PPP model. As aforementioned, the results of cellular uplink networks can not be used in LoRaWANs. To observe the influence of power control on a LoRaWAN uplink, such as the coverage probability, its variance, the proportion of LoRa devices archiving a desired successful probability with a given SIR threshold, we analyse a PPP uplink LoRaWAN with power control in our paper using meta distribution of SIR.

C. Contributions

The main contributions of this paper are summarized as follows:

(a) We discuss the relationship between transmit power and receiver sensitivity considering the thermal noise and present the probability of the received signal strength being greater than the receiver sensitivity. This will guide how the transmit power could be reduced whilst still ensuring acceptable reception.

(b) We derive the coverage probability for uplink LoRaWANs based on a PPP model, and analyse the effect of thermal noise on the coverage probability. The results show that thermal noise can be ignored when analysing the LoRaWANs, because of the high power spectral density.

(c) We derive analytically the b-th moment of SIR for the Poisson LoRaWANs with fractional power control and calculate the meta distribution by beta distribution approximation.

(d) We reveal that power control will benefit the success probability of edge-devices with little effect on the probability of inner-devices if we choose an appropriate power control coefficient. This is different from cellular networks where the success probability of inner-user-equipments is greatly sacrificed to increase the success probability of edge-user-equipments with power control.

The remainder of this paper is organized as follows: We give our system model of LoRaWANs based on Poisson point process in Section II. In Section III, we analyse the coverage probability considering the devices send messages using power control. Exploiting the meta distribution of SIR, more information is revealed in Section IV. The conclusions are given in Section V.

II. System model

We consider an uplink LoRaWAN consisting of GWs and devices, where GWs and devices are randomly deployed according to some homogeneous Poisson point process $\Phi_{\rm g}$ and $\Phi_{\rm d}$ with density $\lambda_{\rm g}$ and $\lambda_{\rm d}$ in a 2-dimensional space as shown in Fig. 1. For simplicity, we assume that all GWs and devices are fixed after deployment for a particular LoRaWAN application, i.e. the information of distances from devices to GWs is well know by GWs and devices. In this case, each device associates with its closest GW (the nearest GW in Euclidean distance) and the fading between the GWs and the devices is Rayleigh fading with unit mean. Using the known distances, devices transmit data with fractional power control (FPC) to save energy. Without loss of generality, we denote GWs and devices by their locations. According to Slivnyak-Mecke theorem [22, Theorem 1.4.5], we consider the typical GW located at the origin, a common device located at x_0, $R = \|x_0\|$ is the Euclidean distance from x_0 to origin. So, the received signal strength from the device x_0 to the typical GW is $P_{\rm tx} h R^{-\alpha}$. $P_{\rm tx}$ is the transmit power of devices x_0. h is the small-scale fading and $h \sim \exp(1)$. $R^{-\alpha}$ is the path loss and $\alpha > 2$ is the path loss exponent. We consider two paradigms, one is that all devices send messages to their tagged GWs with a fixed transmit power $P_{\rm tx} = P_{\rm max}$; the other is that devices send messages to their tagged GWs with FPC, i.e $P_{\rm tx} = P_{\rm s} R^{\alpha\epsilon}$, where $P_{\rm s}$ is the minimum transmit power and defined as the transmit power when R equals the unit distance. $\epsilon \geq 0$ is the fractional power control coefficient. $\epsilon = 0$ defines no power control, $\epsilon = 1$ defines totally compensating path-loss power control and $\epsilon > 1$ defines over-compensating power control.

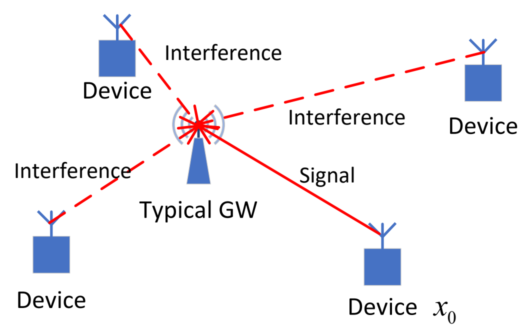

Fig. 1. LoRaWAN uplink model. The typical GW is at the origin, active devices transmit in a same sub-channel with the same SF.

In LoRaWANs, devices communicate with their tagged GWs using a grant-free pure Aloha protocol as the medium access mechanism, which allows multiple devices to send messages simultaneously without any handshaking. LoRaWAN adopts a chirp spread spectrum (CSS) modulation technique to accommodate multiple devices in a single channel. Different spreading factors (SFs) employed by LoRa devices are orthogonal and provide interference immunity at the receiver end [23], [24]. Moreover, LoRa devices enter into sleep to preserve energy when there is no data to send. Each active device (with same SF) transmits data at a randomly chosen sub-channel from total $N_{\rm c}$ channels. Letting $p_{\rm a}$ denote the probability of active devices, then the probability of the active devices simultaneously transmitting data in the same sub-channel with the same SF is $p_{\mathrm{a}}/(N_{\mathrm{c}} \cdot N_{\mathrm{SF}})$, where $N_{\mathrm{SF}} = 6$ (from $SF7$ to $SF12$) is the number of SFs. As shown in Fig. 1, it is worth noting that some interfering devices may be closer to the typical GW than the desired device. This is different from practical cellular downlink scenarios which are best modelled via a soft-core process as a repulsive point process if the typical BS is not considered [25]. In LoRaWAN, according to the thinning theorem [22, Proposition 1.3.5], the set of active devices (with same SF) is still a PPP (Φ_{a}) with density of $\lambda_{\mathrm{a}} = \frac{p_{\mathrm{a}} \cdot \lambda_{\mathrm{d}}}{N_{\mathrm{c}} \cdot N_{\mathrm{SF}}}$.

In very dense deployment scenarios, LoRaWANs will inevitably become interference-limited, rather than noise limited due to the Co-SF interference, caused by other uncoordinated systems using the same SF and channel [23]. In [26], the authors analysed the coverage probability of LoRaWANs considering the influence of thermal noise and Co-SF interference. The results show that the coverage probability is mainly affected by the thermal noise when the devices are far away from the GWs, such as several kilometres. So, whether the thermal noise can be neglected in LoRaWAN should be carefully considered. On the one hand, LoRaWAN devices should transmit data with transmit power as low as possible for power saving because the SIR theoretically will not be influenced by fixed transmit power when neglecting the thermal noise. On the other hand, the receiver will have a minimum sensitivity and will miss the received signal if the transmit power is too low. It is worth knowing how much lower the transmit power can be to ensure the receiver is sensitive to the received signal with the thermal noise not affecting reception.

Definition 1. *In wireless networks, the receiver sensitivity is defined as*

$$\mathrm{RXS} = 10 \log (KTB) + N_{\mathrm{F}} + S_{\mathrm{r}} = P_{\mathrm{N}} + S_{\mathrm{r}}. \qquad (1)$$

Equation (1) is in logarithmic, where K is Boltzmann constant, T is the temperature in Kelvin, B is the bandwidth, and N_{F} is the noise figure. P_{N} is the logarithmic power of noise and S_{r} is the required (predefined) SNR for demodulation at a defined bit error rate.

In wireless networks, receivers work under the condition that the received signal strength is greater than the receiver sensitivity. We measure this performance as the probability that the received signal strength is greater than the receiver sensitivity and it is given as

$$\begin{aligned} \mathbb{P}\left[\frac{P_{\mathrm{tx}} h R^{-\alpha}}{\sigma^2} > \theta\right] &= \mathbb{P}\left[h > \sigma^2 \theta P_{\mathrm{tx}}^{-1} R^{\alpha}\right] \\ &\overset{(a)}{=} \exp\left(-\sigma^2 \theta P_{\mathrm{tx}}^{-1} R^{\alpha}\right), \end{aligned} \qquad (2)$$

where (a) follows from $h \sim \exp(1)$, θ is the linear form of S_{r}. Also note $\sigma^2 = N_{\mathrm{o}} B$ is the linear power of noise, where N_{o} is the power spectral density of noise. In fact, the form in ratio of Eq. (2) is just the probability of received SNR being greater than the required SNR for demodulation.

LoRaWAN devices can work under significant interference because the LoRa signal can be demodulated with a very lower SNR. For example, the minimum required SNR is -20 dB for spreading factor 12 ($SF12$) LoRa signal and -7.5 dB for $SF7$ LoRa signal [27]. This leads to a link budget exceeding 140 dB in LoRaWANs. We consider $P_{\max} = 20$ dBm when a device transmits without power control and $P_{\mathrm{s}} = -20$ dBm when a device transmits with FPC. The bandwidth of each sub-channel is $B = 125$ kHz [28], the noise spectral density $N_{\mathrm{o}} = -173$ dBm/Hz. The typical GW receives signals from a device with distance R. Fig. 2 illustrates how the probability of Eq. (2) changes with the distance R.

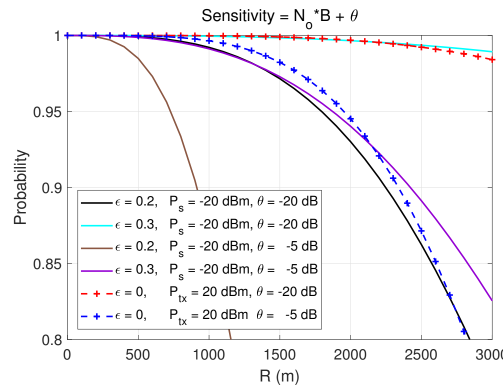

Fig. 2. The probability that received signal strength is larger than the receiver sensitivity varies with the distance. This reveals what the transmit power should be to ensure the reception, for $\alpha = 4$.

As shown in Fig. 2, the probabilities are strongly influenced by the transmit power, required SNR for demodulation, and distance from the device to its tagged GW. For example, when the distance is more than 2 kms, only two lines are close to '1', which represent no power control, $\theta = -20$ dB, and FPC ($\epsilon = 0.3$), $\theta = -20$ dB, respectively. When the distance is less than 1 km and $\epsilon = 0.3$, the probabilities of FPC are always close to '1', although the P_{s} is vary small (-20 dBm). Within a given distance range, we can neglect the thermal noise for all SFs and focus on the $Co-SF$ interference, if the appropriate transmit power is adopted (without power control or with FPC) when we model and analyse the LoRaWANs. This is because LoRa signals can be demodulated at a very low SNR threshold and the power spectral density is very high with lower transmit power but much narrower bandwidth (mostly at 125 kHz for each sub-channel).

Power control can reduce the energy consumption of the devices which are closer to their tagged GWs. Hence it proximity improves transmit power saving. This is very important for LPWAN devices which are mainly powered by batteries. Theoretically, $\epsilon = 1$ means totally compensating the path-loss and statistically all device have the same received signal strength. But a larger ϵ means a wider transmit power range, which may lead to the transmit power of some devices far away from their tagged GWs exceeding the maximum power limit.

For a quick reference, the notations and symbols used in this paper are summarized in the Table I.

III. Coverage probability without power control

It is worth pointing out that the received signal-to-interference-plus-noise ratio (SINR) must be greater than the

TABLE I
NOTATIONS AND SYMBOLS USED IN THE PAPER

Notation	Description
$\Phi_{\rm g}$	The set of gateways
$\Phi_{\rm d}$	The set of devices
$\Phi_{\rm a}$	The set of active devices with same SF
$\Phi_{\rm f}$	The set of interfering devices
$\lambda_{\rm g}$	The density of gateways
$\lambda_{\rm d}$	The density of devices
λ_i	The density of interfering devices
$p_{\rm a}$	The active probability of gateways with same SF
$N_{\rm c}$	The number of total sub-channels
R	Distance from the typical device to its closest GW
R_x	Distance from the device x to its closest GW
D_x	Distance from the device x to the typical GW
$N_{\rm o}$	Power spectral density of Noise
B	The bandwidth
$P_{\rm tx}$	The transmit power of device x
$P_{\rm s}$	The minimum transmit power of devices
$P_{\max}$	The maximum transmit power of devices
α	Path loss exponent
h_x	Small-scale fading
ϵ	coefficient of FPC
S	The area of networks
θ	Required SIR for demodulation

required threshold SINR to demodulate the LoRa signal. The 'N' in SNR of [27] means both thermal noise and interference and so should really be SINR. Eq. (2) and Fig. 2 only consider the influence of thermal noise on sensitivity, coming to the conclusion that thermal noise can be neglected in some cases. In this section, we consider both thermal noise and interference to validate that thermal noise can be ignored and only focus on the interference in a LoRaWAN.

Definition 2. *The coverage probability of LoRaWANs is the probability of the received SINR being greater than the predefined threshold θ, i.e. the standard success probability $p_{\rm s}(\theta) \triangleq \mathbb{P}[{\rm SINR} > \theta]$.*

For our LoRaWAN model, the uplink SINR of the typical GW from the typical device is given by

$$\mathrm{SINR} = \frac{P_{\rm tx} h R^{-\alpha}}{I + \sigma^2}, \tag{3}$$

where $I = \sum_{x \in \Phi_{\rm f}} P_{\rm tx} h_x \|x\|^{-\alpha}$. h_x is the small-scale fading between interfering device x and its tagged GW. We assume all h_x (including h) obey independent and identically distributed (i.i.d) and $h_x \sim \exp(1)$. $D_x = \|x\|$ is the distance from the interfering device x to the typical GW. $\Phi_{\rm f}$ is the set of interfering devices, i.e. all the other active devices except the typical device x_0, denoted as $\Phi_{\rm f} = \Phi_{\rm a} \backslash \{x_{\rm o}\}$. This is different from both the downlink Poisson cellular networks where the typical transmitter (BS) is the closest BS to the user equipment, and the uplink Poisson cellular network where there is at most one user equipment in each cell transmitting in the same RB. In an uplink Poisson LoRaWANs, the typical transmitter (device) can be any one of the devices, and the distance from an interfering device to the receiver (typical GW) may be less than the distance from the wanted transmitter (typical device). Adding $x_{\rm o}$ into $\Phi_{\rm f}$ does not influence on the distribution of $\Phi_{\rm f}$ [22, Chapter 1.4 Palm Theory], i.e. $\Phi_{\rm f}$ is still a PPP with density of $\lambda_{\rm f} = 2 \cdot \lambda_{\rm a} = \frac{2 \cdot p_{\rm a} \cdot \lambda_{\rm d}}{N_{\rm c} \cdot N_{\rm SF}}$ because the collision time is twice the sending cycle in a pure Aloha systems.

Theorem 1. *In LoRaWANs, devices associate with their closest GWs. considering the Rayleigh fading with unit mean, the coverage probability is expressed as*

$$\begin{aligned} p_{\rm s}(\theta) = \int_0^\infty \exp\Big(&-\theta\sigma^2 P_{\rm tx}^{-1} (\lambda_{\rm g}\pi)^{-\alpha/2} z^{\alpha/2} \\ &- \Big(1 + \frac{\lambda_{\rm f}}{\lambda_{\rm g}} \theta^{2/\alpha} f(\alpha)\Big) z\Big) dz, \end{aligned} \tag{4}$$

where

$$f(\alpha) = \int_0^\infty \frac{1}{1 + u^{\alpha/2}} du. \tag{5}$$

$Proof$: According to the definition 2, we have:

$$\begin{aligned} p_{\rm s}(\theta) &= \mathbb{E}\left[\mathbb{P}\left(\frac{P_{\rm tx} h R^{-\alpha}}{I + \sigma^2} > \theta | R\right)\right] \\ &= \mathbb{E}\left[\mathbb{P}\left(h > \left(I + \sigma^2\right) \theta P_{\rm tx}^{-1} R^\alpha | R\right)\right] \\ &\overset{(a)}{=} \mathbb{E}\left[\exp\left(-\sigma^2 \theta P_{\rm tx}^{-1} R^\alpha\right) \mathcal{L}_I(s)\right], \end{aligned} \tag{6}$$

where $s = \theta P_{\rm tx}^{-1} R^\alpha$. The Laplace transform of random variable I in Eq. (6) can be expressed as

$$\begin{aligned} \mathcal{L}_I(s) &= \mathbb{E}_I\left(e^{-sI}\right) \\ &= \mathbb{E}\left[\exp\left(-\theta P_{\rm tx}^{-1} R^\alpha I\right)\right] \\ &= \mathbb{E}\left[\exp\left(-\theta P_{\rm tx}^{-1} R^\alpha \sum_{x \in \Phi_{\rm f}} P_{\rm tx} h_x D_x^{-\alpha}\right)\right] \\ &\overset{(b)}{=} \mathbb{E}\left[\prod_{x \in \Phi_{\rm f}} \frac{1}{1 + \theta D_x^{-\alpha} R^a}\right] \\ &\overset{(c)}{=} \exp\left(-2\lambda_{\rm f}\pi \int_0^\infty \left(1 - \frac{1}{\theta v^{-\alpha} r^\alpha}\right) v dv\right) \\ &= \exp\left(-\lambda_{\rm f}\pi r^2 \theta^{2/\alpha} f(\alpha)\right), \end{aligned} \tag{7}$$

the probability density function (PDF) of R is given as [8]

$$f_R(r) = 2\lambda_{\rm g}\pi r e^{-\lambda_{\rm g}\pi r^2}, \tag{8}$$

where (a) follows from the $h \sim \exp(1)$ and the Laplace transform of PPP. (b) follows from the i.i.d. distribution of $h_x \sim \exp(1)$ and (c) follows from the probability generating functional. Combining Eq. (8) and Eq. (7) with Eq. (6) yields Eq. (4).

Fig. 3 illustrates the influence of noise power density on the coverage probability when the bandwidth of sub-channel $B = 125$ kHz and $\alpha = 4$. The red line denotes the coverage probability when noise is neglected, and it is not influenced by the transmit power theoretically. As shown in Fig. 3, when the transmit power is -10 dBm, the noise has little effect on the coverage probability even $N_o = -160$ dBm/Hz; when the transmit power is -20 dBm and $N_o = -173$ dBm/Hz, the coverage probability (blue dotted line) coincide with the red line; when the transmit power is -20 dBm and $N_o = -160$ dBm/Hz, the coverage probability (cyan dotted line) is still close to the red line with a small gap. So, the thermal noise can be neglected when the transmit power is relatively large.

This is because the bandwidth of LoRaWAN sub-channel is very narrow, it leads to very high power spectral density (even higher than that of cellular networks) although the transmit power is low.

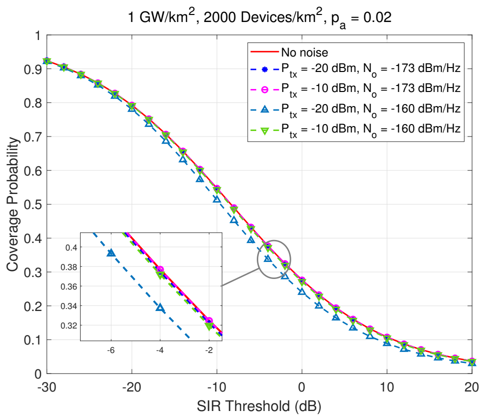

Fig. 3. Coverage probabilities change with the predefined SINR, where $\alpha = 4$ and $N_c = 8$. Dotted lines with marks represent additive noise.

Corollary 1. *The coverage probability of theorem 1 is the spatial averaging of all devices accessing their tagged GWs successfully. To get fine-grained information of devices accessing their tagged GWs successfully, we give the probability of a device with distance R from the origin accessing the typical GW successfully as*

$$p_r(\theta) = \exp\left(-\theta\sigma^2 P_{\mathrm{tx}}^{-1} R^\alpha\right) \mathcal{L}_I\left(\theta P_{\mathrm{tx}}^{-1} R^\alpha\right). \tag{9}$$

In fact, the first term on the right of Eq. (9) equals Eq. (2), i.e. the probability of $\mathbb{P}(\mathrm{SNR} > \theta)$.

IV. Meta distribution of SIR with power control

In order to get more fine-grained information for each individual link in the network, the meta distribution of the SIR is defined by [16] as

$$\overline{F}_{P_s}(x) = \mathbb{P}^o\left(P_s(\theta) > x\right), x \in [0, 1], \tag{10}$$

where $P_s(\theta) \triangleq \mathbb{P}(\mathrm{SIR} > \theta | \Phi)$ is the conditional success probability taken over the fading and the random activities of the interferers, given the point process. $\mathbb{P}^o(\cdot)$ denotes the reduced Palm measure of the point process, given that the receiver is at the origin [7, Definition 8.8].

We focus on the moments of $P_s(\theta)$ because it is most likely impossible to calculate the meta distribution directly from the definition in Eq. (10). The b-th moment of $P_s(\theta)$ is denoted by

$$M_b(\theta) \triangleq \mathbb{E}^o\left(P_s(\theta)^b\right) = \int_0^1 b x^{b-1} \overline{F}_{P_s}(x) dx, b \in \mathbb{C}, \tag{11}$$

where $\mathbb{E}^o(\cdot)$ is the expectation w.r.t. the Palm measure. Hence we easily have the standard success probability $p_s(\theta) \equiv M_1(\theta)$ and the variance of $P_s(\theta)$ equals $M_2(\theta) - M_1^2(\theta)$. The meta distribution of the uplink SIR can be obtained from the Gil-Pelaez theorem [29] as

$$\overline{F}_{P_s}(x) = \frac{1}{2} + \frac{1}{\pi} \int_0^\infty \frac{\mathrm{Im}\left(e^{-jtx} M_{jt}\right)}{t} dt, \tag{12}$$

where $\mathrm{Im}(z)$ denotes the imaginary of the complex number z and $j \triangleq \sqrt{-1}$.

As in [16], some classic bounds and a simple approximation, the beta distribution, were given for the meta distribution of Eq. (12). We only consider the beta distribution approximation in this paper. Since $P_s(\theta)$ is supported on [0,1], it is natural to approximate its distribution with the beta distribution [16]. The PDF of a beta distributed random variable X with mean u is

$$f_X(x) = \frac{x^{\frac{u(\beta+1)-1}{1-u}} (1-x)^{\beta-1}}{B\left(u\beta/(1-u), \beta\right)}, \tag{13}$$

where $B(a, b) = \int_0^1 t^{a-1}(1-t)^{b-1} dt$ is the beta function. The variance is given by

$$\mathrm{var}\ X = \frac{u(1-u)^2}{\beta + 1 - u}. \tag{14}$$

Matching the mean $u = M_1$ and variance $\mathrm{var}\ X = M_2 - M_1^2$ yields

$$\beta = \frac{(1 - M_2)(1 - M_1)}{(M_2 - M_1^2)}. \tag{15}$$

As aforementioned and shown in Fig. 2 and 3, in very dense deployment scenarios, the thermal noise can be neglected when we model and analyse a LoRaWAN if the appropriate transmit power is adopted by each device. In LoRaWAN, the maximum transmit power is 14 dBm in Europe and 27 dBm in the U.S.A. [28]. In this paper, we set the $P_{\mathrm{tx}} = 20$ dBm as a middle value, for simplicity, when LoRaWAN devices transmit data without power control i.e. $\epsilon = 0$; and set $P_{\mathrm{tx}} = P_{\mathrm{s}} R^{\alpha\epsilon}$ when LoRaWAN devices transmit data with power control, where $P_{\mathrm{s}} = -20$ dBm and $\epsilon = 0.3$. This ensures the receivers work properly as shown in Fig. 2 (the received signal strength is greater than the receiver sensitivity with a probability very close to '1'), and the transmit power is in the transmit power range of most LoRaWAN devices. For example, a device with distance 1000 m from its tagged GW will transmit data with power of 16 dBm when $\alpha = 4$ using these settings.

In this section, we focus on the meta distribution of the SIR with FPC. In this case, θ denotes the required SIR for demodulation. The uplink SIR of the typical GW from the typical device with FPC is

$$\mathrm{SIR} = \frac{R^{\alpha(\epsilon-1)} h}{\sum\limits_{x \in \Phi_{\mathrm{f}}} R_x^{\alpha\epsilon} h_x D_x^{-\alpha}}, \tag{16}$$

where R_x is the distance from the interfering device x to its tagged GW.

Remark 1. *According to the strategy that all devices associate with their closest GWs, for any device x, R_x has the same PDF with R and $R_x \le D_x^{-\alpha}$ because the distance from x to its tagged GW is nearer than the distance from x to the typical GW.*

We can easily get the distribution of R_x by conditioning on D_x as

$$f_{R_x|D_x}(r) = \frac{2\lambda_{\mathrm{g}} \pi r e^{-\lambda_{\mathrm{g}} \pi r^2}}{1 - e^{-\lambda_{\mathrm{g}} \pi D_x^2}}. \tag{17}$$

The conditional coverage probability is

$$\begin{aligned} P_{\mathrm{s}}(\theta) &= \mathbb{P}\left(h > \theta \sum_{x\in\Phi_{\mathrm{f}}} h_x R_x^{\alpha\epsilon} D_x^{-\alpha} R^{\alpha(1-\epsilon)} \,|\Phi\right) \\ &= \prod_{x\in\Phi_{\mathrm{f}}} \frac{1}{1+\theta R_x^{\alpha\varepsilon} D_x^{-\alpha} R^{\alpha(1-\varepsilon)}}. \end{aligned} \tag{18}$$

Theorem 2. *In LoRaWANs, the b-th moment of $P_s(\theta)$ of the conditional success probability of uplink with FPC is expressed as*

$$M_b = \int_0^{\infty} \exp\left(-z - f_b\left(b,z\right)\right) dz,\ b\in\mathbb{C}, \tag{19}$$

where

$$\begin{aligned} f_b\left(b,z\right) =& \frac{\lambda_{\mathrm{i}}}{\lambda_{\mathrm{g}}} \int_0^{\infty}\int_0^1 \left(1 - \frac{e^{-xy}}{1-e^{-y}}\right. \\ &\left.\cdot \frac{y}{\left(1+\theta x^{\alpha\epsilon/2} y^{\alpha(\epsilon-1)/2} z^{\alpha(1-\epsilon)/2}\right)^b}\right) dxdy. \end{aligned} \tag{20}$$

Proof:

$$\begin{aligned} M_b =& \mathbb{E}\prod_{x\in\Phi_{\mathrm{f}}} \frac{1}{\left(1+\theta\frac{R_x^{\alpha}R^{\alpha(1-\epsilon)}}{D_x^{\alpha}}\right)^b} \\ =& \mathbb{E}\prod_{x\in\Phi_{\mathrm{f}}} \mathbb{E}_{R_x}\left(\frac{1}{\left(1+\theta\frac{R_x^{\alpha}R^{\alpha(1-\epsilon)}}{D_x^{\alpha}}\right)^b}\,|D_x,R\right) \\ =& \mathbb{E}\prod_{x\in\Phi_{\mathrm{f}}} \int_0^{D_x} \frac{2\pi\lambda_{\mathrm{g}} t e^{-\lambda_{\mathrm{g}}\pi t^2}}{1-e^{-\lambda_{\mathrm{g}}\pi D_x^2}} \frac{1}{\left(1+\theta t^{\alpha\epsilon} D_x^{-\alpha} R^{\alpha(1-\epsilon)}\right)^b} dt \\ \overset{(a)}{=}& \mathbb{E}_R \exp\left(-2\lambda_{\mathrm{f}}\pi \int_0^1 \left(1 - \int_0^v \frac{2\pi\lambda_{\mathrm{g}} t e^{-\lambda_{\mathrm{g}}\pi t^2}}{1-e^{-\lambda_{\mathrm{g}}\pi v^2}}\right.\right. \\ &\left.\left.\cdot \frac{1}{\left(1+\theta t^{\alpha\epsilon} v^{-\alpha} R^{\alpha(1-\epsilon)}\right)^b} dt\right) vdv\right) \\ =& \int_0^{\infty} 2\pi\lambda_{\mathrm{g}} r \exp\left(-2\lambda_{\mathrm{f}}\pi \int_0^{\infty}\left(1 - \int_0^v \frac{2\pi\lambda_{\mathrm{g}} t e^{-\lambda_{\mathrm{g}}\pi t^2}}{1-e^{-\lambda_{\mathrm{g}}\pi v^2}}\right.\right. \\ &\left.\left.\cdot \frac{1}{\left(1+\theta t^{\alpha\epsilon} v^{-\alpha} r^{\alpha(1-\epsilon)}\right)^b} dt\right) vdv\right) e^{-\lambda_{\mathrm{g}}\pi r^2} dr, \end{aligned} \tag{21}$$

where (a) follows from the probability generating functional of PPP. Letting $\lambda_{\mathrm{g}}\pi t^2 = x$, $\lambda_{\mathrm{g}}\pi v^2 = w$, $y = t/v$, $\lambda_{\mathrm{g}}\pi r^2 = z$ yields Eq. (19).

Corollary 2. *Based on Theorem 2, let $b=1$, the probability of a device with distance R from the origin successfully accessing the typical GW with FPC is then given as*

$$p_r\left(\theta\right) = e^{-f_b\left(1,\lambda_{\mathrm{g}}\pi R^2\right)}. \tag{22}$$

Fig. 4 shows how the first moment, i.e. the standard success probability and the variance of the conditional coverage probability vary with the required SIR when FPC coefficient $\epsilon = 0.3$ and path loss exponent $\alpha = 4$. To validate our numerical results, we compare them with Monte Carlo simulations. In each simulation, 25 ($1\ \mathrm{GW/km^2}$) GWs and 50,000 devices ($2000\ \mathrm{devices/km^2}$) are randomly deployed following the PPP in a $5\mathrm{km}\times 5\mathrm{km}$ square range and the tagged GW is located at the origin. The values of other parameters are produced by the simulation as numerical results. The loop of Monte Carlo simulation is 10,000. The purple dotted line with marks correspond to simulation results. With power control, the coverage probability (M_1) in the high-θ regime is lower than the coverage probability without power control. In the low-θ regime, coverage probability is also higher than the coverage probability without power control. This is because power control balances the success probability in whole networks by sacrificing the good-link devices (mostly, the inner-devices) to compensate the bad-link devices (mostly, the edge-devices). This can be proved by considering the variance of the conditional coverage probability, which is lower when devices transmit data with power control than that when devices transmit data without power control because power control reduces the difference between the individual links, resulting in better fairness.

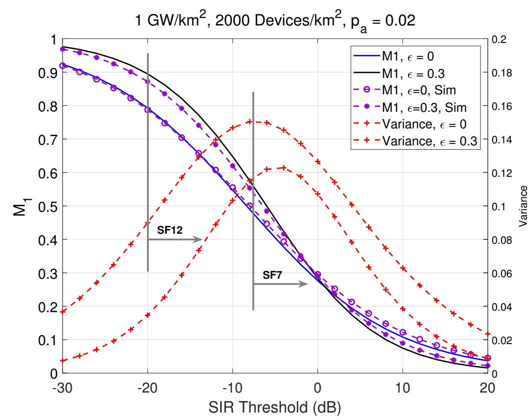

Fig. 4. Comparison of M_1 and variance of $P_{\mathrm{s}}(\theta)$ for no power control $\epsilon = 0$, and power control $\epsilon = 0.3$, where $\alpha = 4$, and $N_{\mathrm{c}} = 8$. Purple dotted line with marks correspond to simulation results.

In uplink cellular networks, the dencities of users and BSs do not influence the successful probability of users because there is only one user transmits data to its tagged BS and other interfering users are far from the considered user's tagged BS. In LoRaWAN, any device randomly starts a transmission leading to the success probability of devices is mainly affected by the active probability of devices p_{a} and the density of GWs. Moreover, in uplink cellular networks, the required SIR for demodulation is very high, to support user transmit data with high baud rate. A smaller FPC coefficient ϵ will lead to larger reduction of success probability of inner-devices. In LoRaWANs, the LoRa signal can be demodulated at very lower SIR threshold (-20 dB for $SF12$ LoRa modulation signal). As shown in Fig. 4, the coverage probability with FPC increases comparing to that without power control even when $\theta = -7.5$ dB, which is the minimum required SIR threshold for $SF7$ LoRa signal. This means the average success probability of the whole network increases while the success probability of edge-devices increases, and the FPC has little effect on inner-device.

Fig. 5 illustrates the success probability as a function of the distance from devices to their tagged GWs when the FPC coefficient $\epsilon = 0.3$ and the loss exponent $\alpha = 4$.

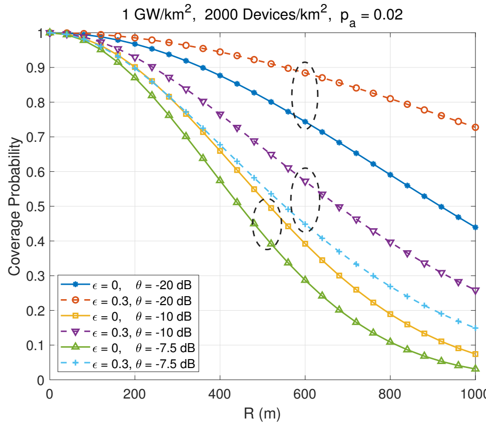

Fig. 5. The probability of a device with distance R from the origin successfully accessing its tagged GW when neglecting the noise and $N_c = 8$.

As shown in Fig. 5, power control strongly influences the probability when the SIR threshold $\theta = -20$ dB but only lightly influences the probability when the SIR threshold $\theta = -7.5$ dB. This is because when $\theta = -20$ dB and $\theta = -7.5$ dB the required SIR thresholds for demodulation are circa 0.01 and 0.178, respectively. The smaller value of SIR threshold is more readily achieved across the nodes when power control is implemented.

Furthermore, the proportion of devices with a given success probability can be obtained with the aid of the meta distribution of SIR. Fig. 6 shows the meta distribution from both the beta distribution approximation and simulation result when $\theta = -10$ dB and $\alpha = 4$.

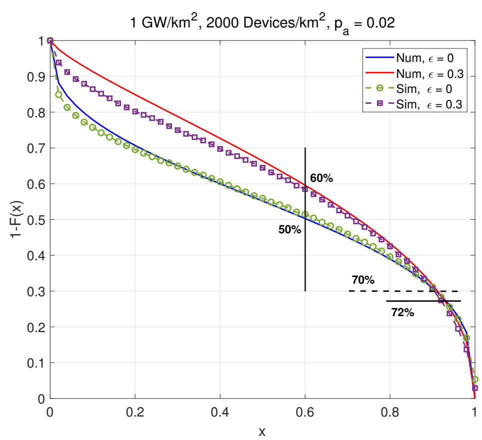

Fig. 6. The simulated meta distribution and the beta approximation, where $\epsilon = 0.3$, $\theta = -10$ dB, $\alpha = 4$ and $N_c = 8$.

As shown in Fig. 6, for example, there are about 50% of devices with a success probability (received SIR greater than -10 dB) is greater than 60% ($x = 0.6$) when $\epsilon = 0$; the number of devices reaches 60% when $\epsilon = 0.3$. Moreover, about 70% ($F(x)$, 72% Numerical) of devices' success probabilities significantly increase at the expense of a very small reduction of the remaining devices' success probabilities. The maximum reduction is less than 4%. This means power control can greatly benefit the edged-devices with little effect on the inner-devices if an appropriate ϵ is adopted.

V. Conclusions

In this paper, we utilize meta distribution to analyse the LoRaWANs based on the Poisson point process model. We discussed the relationship between transmit power and receiver sensitivity. Each device must transmit data with a very high power to ensure the received signal strength is greater than the receiver sensitivity, when power control is not used. Comparatively, with power control, the received signal strength is greater than the receiver sensitivity with a very high probability even if devices transmit data with much lower power. For example, the inner-devices can transmit with -20 dBm and the probability of received signal strength being greater than the receiver sensitivity is still very close to '1'.

Then, we derived the coverage probability of LoRaWANs, the numerical and simulation results show the noise can be neglecting although the transmit power is small but the power spectral density is very high due to vary narrow bandwidth. Applying the b-th moment of the conditional coverage probability, and Beta distribution approximation, we found the meta distribution of SIR for uplink LoRaWANs with power control. The numerical and simulation results show that the coverage probabilities of edge-devices have been greatly improved at the small expense of coverage probabilities of inner-devices with power control. Moreover, the meta distribution of SIR can reveal more information about the individual link distribution in a LoRaWAN realization.

References

[1] J. Gantz and D. Reinsel, "The digital universe in 2020: Big data, bigger digital shadows, and biggest growth in the far east," *IDC iView: IDC Analyze the Future*, pp. 1–16, 2012.

[2] S. Taylor, "The next generation of the Internet revolutionizing the way we work, live, play, and learn," *CISCO Point of View*, 2013.

[3] A. Zanella, N. Bui, A. Castellani, L. Vangelista, and M. Zorzi, "Internet of Things for smart cities," *IEEE Internet of Things Journal*, vol. 1, no. 1, pp. 22–32, 2014.

[4] A. Al-Fuqaha, m. guizani, M. Mohammadi, M. Aledhari, and M. Ayyash, "Internet of Things: A survey on enabling technologies, protocols and applications," *IEEE Communications Surveys & Tutorials*, vol. 17, no. 4, pp. 2347–2376, 2015.

[5] J. Lin, W. Yu, N. Zhang, X. Yang, H. Zhang, and W. Zhao, "A survey on Internet of Things: architecture, enabling technologies, security and privacy, and applications," *IEEE Internet of Things Journal*, vol. 4, no. 5, pp. 1125–1142, 2017.

[6] "Narrowband Internet of Things," Whitepape, 3GPP, August 2016.

[7] M. Haenggi, *Stochastic geometry for wireless networks*. Cambridge University Press, 2012.

[8] J. G. Andrews, F. Baccelli, and R. K. Ganti, "A tractable approach to coverage and rate in cellular networks," *IEEE Transactions on Communications*, vol. 59, no. 11, pp. 3122–3134, 2011.

[9] H. S. Dhillon, R. K. Ganti, F. Baccelli, and J. G. Andrews, "Modeling and analysis of k-tier downlink heterogeneous cellular networks," *IEEE Journal on Selected Areas in Communications*, vol. 30, no. 3, pp. 550–560, 2012.

[10] T. D. Novlan, H. S. Dhillon, and J. G. Andrews, "Analytical modeling of uplink cellular networks," *IEEE Transactions on Wireless Communications*, vol. 12, no. 6, pp. 2669–2679, 2013.

[11] S. Singh, X. Zhang, and J. G. Andrews, "Joint rate and SINR coverage analysis for decoupled uplink-downlink biased cell associations in HetNets," *IEEE Transactions on Wireless Communications*, vol. 14, no. 10, pp. 5360–5373, 2014.

[12] X. Zhang and M. Haenggi, "Cellular network coverage with inter-cell interference coordination and intra-cell diversity," in *2014 IEEE International Symposium on Information Theory*, June 2014, pp. 996–1000.

[13] B. Blaszczyszyn and P. Muehlethaler, "Interference and SINR coverage in spatial non-slotted Aloha networks," *Ann. Telecommunications*, vol. 70, no. 7-8, pp. 345–358, 2015.

[14] V. Naghshin, M. C. Reed, S. V. Hanly, and N. Aboutorab, "Downlink coverage analysis of two-tier heterogeneous networks with asynchronous slots," in *2016 IEEE International Conference on Communications (ICC)*, 2016, pp. 1–6.

[15] H. Hu, J. Weng, and J. Zhang, "Coverage performance analysis of feicic low-power subframes," *IEEE Transactions on Wireless Communications*, vol. 15, no. 8, pp. 5603–5614, 2016.

[16] M. Haenggi, "The meta distribution of the SIR in Poisson bipolar and cellular networks," *IEEE Transactions on Wireless Communications*, vol. 15, no. 4, pp. 2577–2589, 2016.

[17] Z. Li, S. Zozor, J. M. Drossier, N. Varsier, and Q. Lampin, "2D time-frequency interference modelling using stochastic geometry for performance evaluation in low-power wide-area networks," in *IEEE International Conference on Communications*, 2017, pp. 1–7.

[18] F. Baccelli, B. Blaszczyszyn, and P. Muhlethaler, "Stochastic analysis of spatial and opportunistic aloha," *IEEE Journal on Selected Areas in Communications*, vol. 27, no. 7, pp. 1105–1119, 2009.

[19] K. Higuchi, Y. Saito, and S. Nakao, "Inter-cell interference coordination using coordinated inter-cell interference power control in uplink," in *International Conference on Signal Processing and Communication Systems*, 2015, pp. 1–5.

[20] H. Elsawy and E. Hossain, "On stochastic geometry modeling of cellular uplink transmission with truncated channel inversion power control," *IEEE Transactions on Wireless Communications*, vol. 13, no. 8, pp. 4454–4469, 2014.

[21] Y. Wang, M. Haenggi, and Z. Tan, "The meta distribution of the SIR for cellular networks with power control," *IEEE Transactions on Communications*, vol. 66, no. 4, pp. 1745–1757, 2018.

[22] F. Baccelli and B. Błaszczyszyn, *Stochastic geometry and wireless networks: Volume I Theory*. Now Publishers, 2009.

[23] O. Georgiou and U. Raza, "Low power wide area network analysis: Can LoRa scale?" *IEEE Wireless Communications Letters*, vol. 6, no. 2, pp. 162–165, 2017.

[24] J. T. Lim and Y. Han, "Spreading factor allocation for massive connectivity in LoRa systems," *IEEE Communications Letters*, vol. 22, no. 4, pp. 800–803, 2018.

[25] M. Haenggi, "User point processes in cellular networks," *IEEE Wireless Communications Letters*, vol. 6, no. 2, pp. 258–261, 2017.

[26] A. Mahmood, E. G. Sisinni, L. Guntupalli, R. Rondón, and M. Gidlund, "Scalability analysis of a LoRa network under imperfect orthogonality," *IEEE Transactions on Industrial Informatics*, vol. 15, no. 3, pp. 1425–1436, 2018.

[27] "SX1276/77/78/79 data sheet," Semtech Corporation, March 2015.

[28] *LoRaWAN 1.0.2 regional parameters*, LoRa Alliance Standard, 2017.

[29] J. Gil-Pelaez, "Note on the inversion theorem," *Biometrika*, vol. 38, no. 3/4, pp. 481–482, 1951.